Volatile and Organic Compositions of Sedimentary Rocks in Yellowknife Bay, Gale Crater, Mars

D. W. Ming *et al.*

Science **343**, (2014);
DOI: 10.1126/science.1245267

Science (print ISSN 0036-8075; online ISSN 1095-9203) is published weekly, except the last week in December, by the American Association for the Advancement of Science, 1200 New York Avenue NW, Washington, DC 20005.

Volatile and Organic Compositions of Sedimentary Rocks in Yellowknife Bay, Gale Crater, Mars

D. W. Ming,[1]* P. D. Archer Jr.,[2] D. P. Glavin,[3] J. L. Eigenbrode,[3] H. B. Franz,[3,4] B. Sutter,[2] A. E. Brunner,[3,5] J. C. Stern,[3] C. Freissinet,[3,6] A. C. McAdam,[3] P. R. Mahaffy,[3] M. Cabane,[7] P. Coll,[8] J. L. Campbell,[9] S. K. Atreya,[10] P. B. Niles,[1] J. F. Bell III,[11] D. L. Bish,[12] W. B. Brinckerhoff,[3] A. Buch,[13] P. G. Conrad,[3] D. J. Des Marais,[14] B. L. Ehlmann,[15,16] A. G. Fairén,[17] K. Farley,[15] G. J. Flesch,[16] P. Francois,[8] R. Gellert,[9] J. A. Grant,[18] J. P. Grotzinger,[15] S. Gupta,[19] K. E. Herkenhoff,[20] J. A. Hurowitz,[21] L. A. Leshin,[22] K. W. Lewis,[23] S. M. McLennan,[21] K. E. Miller,[24] J. Moersch,[25] R. V. Morris,[1] R. Navarro-González,[26] A. A. Pavlov,[3] G. M. Perrett,[9] I. Pradler,[9] S. W. Squyres,[17] R. E. Summons,[24] A. Steele,[27] E. M. Stolper,[15] D. Y. Sumner,[28] C. Szopa,[8] S. Teinturier,[8] M. G. Trainer,[3] A. H. Treiman,[29] D. T. Vaniman,[30] A. R. Vasavada,[16] C. R. Webster,[16] J. J. Wray,[31] R. A. Yingst,[30] MSL Science Team†

H_2O, CO_2, SO_2, O_2, H_2, H_2S, HCl, chlorinated hydrocarbons, NO, and other trace gases were evolved during pyrolysis of two mudstone samples acquired by the Curiosity rover at Yellowknife Bay within Gale crater, Mars. H_2O/OH-bearing phases included 2:1 phyllosilicate(s), bassanite, akaganeite, and amorphous materials. Thermal decomposition of carbonates and combustion of organic materials are candidate sources for the CO_2. Concurrent evolution of O_2 and chlorinated hydrocarbons suggests the presence of oxychlorine phase(s). Sulfides are likely sources for sulfur-bearing species. Higher abundances of chlorinated hydrocarbons in the mudstone compared with Rocknest windblown materials previously analyzed by Curiosity suggest that indigenous martian or meteoritic organic carbon sources may be preserved in the mudstone; however, the carbon source for the chlorinated hydrocarbons is not definitively of martian origin.

Curiosity landed in Gale crater on 6 August 2012 (UTC) with a goal to explore and quantitatively assess a site on Mars' surface as a potential habitat for past or present life. A topographic low informally named Yellowknife Bay located about 0.5 km northeast of the landing site was chosen as the first major exploration target because strata exposed were inferred to be fluvio-lacustrine deposits (*1*). Fluvio-lacustrine depositional systems are thought to preserve measurable evidence of paleo-habitability (*2*), e.g., factors such as mineral associations, elemental inventory, redox state, and character of light elements and compounds.

Curiosity entered Yellowknife Bay on sol 125 (12 December 2012) and began a drilling campaign to obtain powder samples from a mudstone located near the base of an exposed stratal succession (*3*, *4*). Two drill samples informally named John Klein (drilled on sol 183) and Cumberland (drilled on sol 279) were extracted for delivery to the Sample Analysis at Mars (SAM) (*5*) and Chemistry and Mineralogy (CheMin) (*6*) instruments. The samples were obtained from the lowermost stratigraphic unit in the Yellowknife Bay formation, informally named the Sheepbed member (*1*). The Sheepbed member and an overlying medium- to coarse-grained sandstone, named the Gillespie Lake member, appear to have a complex postdepositional aqueous history. Apparent low matrix permeability in these units suggests that they were lithified during an early diagenetic event followed by at least one additional aqueous episode when Ca-sulfate minerals precipitated in a network of intersecting fractures (*7*). Millimeter-sized nodules and hollow nodules in the Sheepbed member are interpreted, respectively, to be concretions and void spaces possibly formed as trapped gas bubbles during early diagenesis and lithification (*1*). The geology, stratigraphy, and diagenetic history of Yellowknife Bay are described in detail in companion papers (*1*, *7*, *8*).

The John Klein (JK) and Cumberland (CB) targets were drilled about 3 m apart in the Sheepbed mudstone and within ≈10 cm of the same stratigraphic position. The JK drill hole intersected thin Ca-sulfate–rich veins. The CB sample was collected from an area rich in nodules and poor in Ca-sulfate–rich veins, to aid in mineralogical and geochemical characterization of the nodules. Powders extracted from both holes were gray in color, suggesting a relatively unoxidized material (*1*, *8*), in contrast to the red-colored, oxidized materials observed earlier by Curiosity at the Rocknest aeolian deposit (*9*, *10*) and other surface soils (*11*) encountered by previous missions (*12*). Additional details on the drill holes are described in (*1*) and (*8*), including maps of light-toned fractures in the drill hole walls (*8*).

Here we describe the volatile and organic C content of the Sheepbed mudstone and evaluate its potential for preservation of organic C. Volatile-bearing phases (including possible organic material) in Sheepbed are indicators of its past environmental and geochemical conditions and can shed light on whether the environment recorded in this mudstone once was habitable, i.e., met the requirements for microbial life as known on Earth (*13*). The volatile and organic compositions of JK and CB materials were characterized by the SAM instrument's evolved gas analysis (EGA), gas chromatography–mass spectrometry (GCMS), and tunable laser spectroscopy (TLS) experiments (*14*). Four JK subsamples (JK-1, JK-2, JK-3, and JK-4) and four CB subsamples (CB-1, CB-2, CB-3, and CB-5) of the <150-μm-size fraction of drill fines were delivered to SAM for EGA and GCMS analyses (*15*).

Evolved H_2O

The most abundant gas evolved from JK and CB materials was H_2O. H_2O abundances released from JK [1.8 to 2.4 weight percent (wt %) H_2O] and CB (1.7 to 2.5 wt % H_2O; Table 1) were similar to those of Rocknest (1.6 to 2.4 wt % H_2O)

[1]Astromaterials Research and Exploration Science Directorate, NASA Johnson Space Center, Houston, TX 77058, USA. [2]Jacobs, Houston, TX 77058, USA. [3]Planetary Environments Laboratory, NASA Goddard Space Flight Center, Greenbelt, MD 20771, USA. [4]Center for Research and Exploration in Space Science and Technology, University of Maryland Baltimore County, Baltimore, MD 21250, USA. [5]Center for Research and Exploration in Space Science and Technology, Department of Astronomy, University of Maryland, College Park, MD 20742, USA. [6]NASA Postdoctoral Program, NASA Goddard Space Flight Center, Greenbelt, MD 20771, USA. [7]Laboratoire Atmospheres, Milieux, Observations Spatiales, Univ. Pierre Marie Curie, Univ. Paris 06, Université Versailles St-Quentin, UMR CNRS 8970, 75005 Paris, France. [8]Laboratoire Interuniversitaire des Systèmes Atmosphériques, Univ. Paris-Est Créteil, Univ. Paris Diderot and CNRS, 94000 Créteil, France. [9]Department of Physics, University of Guelph, Guelph, Ontario, Canada N1G2W1. [10]Department of Atmospheric, Oceanic and Space Sciences, University of Michigan, Ann Arbor, MI 48109–2143, USA. [11]School of Earth and Space Exploration, Arizona State University, Tempe, AZ 85287, USA. [12]Department of Geological Sciences, Indiana University, Bloomington, IN 47405, USA. [13]Laboratoire de Génie des Procédés et les Matériaux, Ecole Centrale Paris, 92295 Chatenay-Malabry, France. [14]Department of Space Sciences, NASA Ames Research Center, Moffett Field, CA 94035, USA. [15]Division of Geologic and Planetary Sciences, California Institute of Technology, Pasadena, CA 91125, USA. [16]Jet Propulsion Laboratory, California Institute of Technology, Pasadena, CA 91109, USA. [17]Department of Astronomy, Cornell University, Ithaca, NY 14853, USA. [18]Center for Earth and Planetary Studies, National Air and Space Museum, Smithsonian Institution, Washington, DC 20560, USA [19]Department of Earth Science and Engineering, Imperial College London, London SW7 2AZ, UK. [20]U.S. Geological Survey, Flagstaff, AZ 86001, USA. [21]Department of Geosciences, State University of New York State at Stony Brook, NY 11794–2100, USA. [22]Department of Earth and Environmental Science and School of Science, Rensselaer Polytechnic Institute, Troy, NY 12180, USA. [23]Princeton University, Princeton, NJ 08544, USA. [24]Department of Earth, Atmospheric and Planetary Sciences, Massachusetts Institute of Technology, Cambridge, MA 02139, USA. [25]Department of Earth and Planetary Sciences, University of Tennessee, Knoxville, TN 37996, USA. [26]Instituto de Ciencias Nucleares, Universidad Nacional Autónoma de México, Ciudad Universitaria, México D.F. 04510, Mexico. [27]Geophysical Laboratory, Carnegie Institution of Washington, Washington, DC 20015, USA. [28]Department of Earth and Planetary Sciences, University of California, Davis, CA 95616, USA. [29]Lunar and Planetary Institute, Houston, TX 77058, USA. [30]Planetary Science Institute, Tucson, AZ 85719, USA. [31]School of Earth and Atmospheric Sciences, Georgia Institute of Technology, Atlanta, GA 30332, USA.

*Corresponding author. E-mail: douglas.w.ming@nasa.gov
†MSL Science Team authors and affiliations are listed in the supplementary materials.

(*10*). Other major evolved gases, in descending order of abundance, were H_2, CO_2, SO_2, and O_2 from JK and H_2, O_2, CO_2, and SO_2 from CB (Table 1 and Figs. 1 and 2).

An independent estimate of the volatile inventory of JK and CB can be obtained from measurements made by the Alpha Particle X-ray Spectrometer (APXS) (*16*). The measurement calculates the bulk concentration of the aggregate of excess light elements (including H_2O, CO_2, C, F, B_2O_3 and Li_2O) using the relative intensities of Compton- and Rayleigh-scattering peaks (*14*, *17*). Estimates of the average excess light-element concentrations for the JK drill tailings (APXS measurement on sol 230) and the CB drill tailings (sol 287) were 4.3 (±5.5) and 6.9 (±6.2) wt %, respectively. The two methods for determining volatile abundances in the mudstone are consistent within uncertainties.

The JK and CB samples showed similar releases of H_2O in EGA experiments with a continuous temperature ramp (Figs. 1A and 2A) (*18*, *19*). Evolved H_2O from JK (JK-4) resulted in two major H_2O releases, with very broad peaks at about 160° and 725°C (Fig. 1A). Cumberland samples exhibited similar behavior (Fig. 2A). The majority (~70%) of H_2O was driven off in the lower-temperature peak.

CheMin results constrain the potential phases releasing H_2O in the lower peak in JK and CB samples. CheMin detected basaltic silicate minerals (feldspar, pyroxene, olivine), magnetite (maghemite), anhydrite, bassanite, akaganeite, sulfides, and ~30 wt % x-ray amorphous components in addition to a 2:1 trioctahedral phyllosilicate in JK and CB (*8*). Therefore, candidates for the lower-temperature water release are H_2O adsorbed on grain surfaces, interlayer H_2O associated with exchangeable cations in 2:1 phyllosilicates (e.g., smectite), structural H_2O (e.g., bassanite), structural OH (e.g., Fe-oxyhydroxides such as akaganeite), and occluded H_2O in glass or minerals. Adsorbed H_2O and interlayer H_2O in 2:1 phyllosilicates will generally release water below 300°C. Bassanite ($CaSO_4{\cdot}½H_2O$) dehydrates at ~150°C. Akaganeite [FeO(OH,Cl)] undergoes dehydroxylation at ~250°C (fig. S2). H_2O incorporated into the amorphous components (e.g., nanophase Fe-oxides, allophane/hisingerite) may also evolve below 450°C. Water as liquid or vapor inclusions in glass or minerals would be released over a wide range of temperatures. Additional sources of evolved H_2O at low temperatures not constrained by CheMin include structural H_2O in oxychlorine compounds (e.g., hydrated perchlorates), structural OH in organics, and H_2O formed during organic reactions in the SAM pyrolysis oven. Organic matter can release H_2O over a wide range of temperatures from structural O and H as a consequence of reactions that take place in the SAM oven.

The high-temperature H_2O release between 450° and 835°C is consistent with the dehydroxylation of the octahedral layer of a 2:1 phyllosilicate (e.g., smectite), although other phases that contain OH in octahedral layers may also evolve H_2O in this temperature region. The basal (001) spacing of the JK phyllosilicate measured by CheMin was mostly collapsed to ~10 Å suggesting a 2:1 phyllosilicate with little interlayer H_2O (*8*). The 2:1 phyllosilicate in the CB sample was expanded, with a basal (001) spacing of ~13 to 14 Å, consistent with several possible interpretations; the CB phyllosilicate could be smectite with an interlayer partially occupied by metal-hydroxyl groups or smectite with high–hydration-energy cations (e.g., Mg^{2+}), facilitating retention of H_2O (*8*). The high-temperature H_2O releases at 750°C can be ascribed to dehydroxylation of Mg- and Al-enriched octahedral sheets in 2:1 phyllosilicates (Fig. 3A). The most likely candidate for the high-temperature H_2O release (i.e., ~750°C) in Sheepbed material is saponite or Fe-saponite based on CheMin measurement of the 02ℓ diffraction band (4.58 Å) as consistent with a trioctahedral 2:1 phyllosilicate (*8*) and the water-release peak temperature (Fig. 3A). If all of the H_2O released between 450° and 835°C during SAM pyrolysis runs resulted from dehydroxylation of 2:1 phyllosilicates, the proportions of 2:1 phyllosilicate present in the JK and CB samples are 17 (±12) wt % and 16 (±11) wt %, respectively. These values are consistent with the independent estimates from CheMin x-ray diffraction semiquantitative data, which give 22 (±11) and 18 (±9) wt % for 2:1 phyllosilicate in JK and CB, respectively (*8*).

High-temperature release of H_2 occurs over roughly the same temperature regions as the high-temperature releases of H_2O and H_2S (Figs. 1

Table 1. Evolved gas abundances released during SAM pyrolysis runs of samples (<150 μm fraction) obtained from the John Klein and Cumberland drill holes. Rocknest aeolian material evolved gas abundances are provided for comparison with the Sheepbed mudstone materials.

	John Klein				Cumberland			CB- 5	Rocknest† Average of four runs
	JK-1	JK-2	JK-3*	JK- 4	CB-1	CB-2	CB-3		
					Molar abundances (μmol)				
H_2O	57.4 ± 32.7‡	54.2 ± 30.8	59.9 ± 33.7	44.7 ± 25.0	42.7 ± 28.8	54.0 ± 29.5	62.4 ± 31.5	45.0 ± 25.4	55.1 ± 35.3
CO_2	7.0 ± 1.9	8.1 ± 1.7	6.6 ± 1.6	5.7 ± 1.3	2.0 ± 0.5	2.5 ± 0.7	3.1 ± 0.6	3.1 ± 0.7	9.9 ± 1.2
SO_2	1.6 ± 0.6	1.4 ± 0.1	2.9 ± 0.1	2.0 ± 0.0	0.4 ± 0.02	1.3 ± 0.2	1.2 ± 0.2	1.4 ± 0.2	12.2 ± 0.9
O_2	0.6 ± 0.1	0.8 ± 0.1	2.1 ± 0.3	0.9 ± 0.1	2.6 ± 0.3	8.4 ± 1.0	9.9 ± 1.2	11.2 ± 1.4	3.9 ± 0.2
H_2	9.3 ± 1.8	5.1 ± 1.0	4.9 ± 0.9	5.3 ± 1.0	6.9 ± 1.3	11.6 ± 2.2	4.3 ± 0.8	4.1 ± 0.8	Not measured directly
					High-temperature H_2O (%)§				
	21 ± 8	21 ± 8	26 ± 9	34 ± 11	26 ± 26	31 ± 8	19 ± 1	31 ± 11	
					Molar abundances (nmol)				
HCl	58.5 ± 26.1	72.4 ± 32.2	536.1 ± 238.7	155.1 ± 69.1	44.1 ± 19.6	179.9 ± 80.1	267.7 ± 119.2	584.9 ± 260.5	36.5 ± 10.4
H_2S	79.0 ± 35.2	57.0 ± 25.4	95.2 ± 42.4	36.1 ± 16.1	18.7 ± 8.3	67.4 ± 30.0	38.9 ± 17.3	34.4 ± 15.3	61.0 ± 13.9
NO	190 ± 38	188 ± 38	162 ± 32	129 ± 26	190 ± 38	331 ± 66	389 ± 78	374 ± 75	175 ± 40
					Sample weight (%)				
H_2O	2.3 ± 1.6	2.2 ± 1.5	2.4 ± 1.5	1.8 ± 1.2	1.7 ± 1.3	2.2 ± 1.5	2.5 ± 1.6	1.8 ± 1.2	2.0 ± 1.3
CO_2	0.7 ± 0.3	0.8 ± 0.4	0.6 ± 0.2	0.6 ± 0.3	0.2 ± 0.09	0.2 ± 0.1	0.3 ± 0.1	0.3 ± 0.1	0.9 ± 0.1
SO_3 equiv.	0.3 ± 0.1	0.2 ± 0.1	0.5 ± 0.12	0.4 ± 0.1	0.1 ± 0.0	0.2 ± 0.1	0.2 ± 0.09	0.2 ± 0.10	2.0 ± 0.2
Cl_2O_7 equiv.	0.07 ± 0.03	0.09 ± 0.04	0.24 ± 0.06	0.10 ± 0.04	0.3 ± 0.1	1.0 ± 0.4	1.2 ± 0.5	1.3 ± 0.5	0.4 ± 0.1

*Three sample portions (~135 ± 31 mg) of John Klein drill material were delivered to SAM for the JK-3 experimental run. The numbers in this column have been normalized to one sample portion (45 mg). †Average of four SAM runs of the Rocknest aeolian material (*10*). ‡ Errors reported for molar abundances of CO_2, SO_2, and O_2 are the 2σ standard deviation from the mean of calculations done with different *m/z* values for the same species. H_2O error bars are based on the uncertainty in prelaunch water abundance calibration. Errors for other species include the uncertainty in differences in ionization efficiency between masses with a calibrated mol/counts value and uncalibrated values (*10*). Weight % values were calculated with an estimated sample mass of 45 ± 18 mg (2σ), with errors propagated including the uncertainty in molar abundance (*10*). §High-temperature H_2O is the percentage of the H_2O released between 450° and 835°C, which is the temperature region for dehydroxylation of a 2:1 phyllosilicate, compared to the total H_2O released. Errors are the 2σ standard deviation from the mean.

and 2). The origin of the high-temperature evolved H_2 is unknown but is likely associated with the dehydroxylation of the most thermally stable OH groups in the 2:1 phyllosilicates.

Evolved O_2

The JK and CB samples have distinctly different O_2 releases (Figs. 1A and 2A and Table 1). The onset of O_2 evolution from JK (~150°C) was lower than for CB (~230°C). O_2 abundances released from CB (0.3 to 1.3 wt % Cl_2O_7) were nearly eight times the abundances for JK (0.07 to 0.24 wt % Cl_2O_7); Rocknest O_2 abundances (0.4 wt. % Cl_2O_7) were about four times those for JK (Table 1). By comparison, the perchlorate anion (ClO_4^-) was present in soil at the Phoenix landing site at the 0.4 to 0.6 wt % level (*20*). The JK-4 sample had two distinct peaks, suggesting different or additional O_2-evolving phases in the JK sample or consumption of O_2 during combustion of organic materials (see below) or thermal oxidation of ferrous-containing phases (e.g., magnetite to maghemite transition). O_2 evolution in the Rocknest aeolian material occurred at a higher temperature (onset ~300°C with a peak temperature ~400°C) than in JK and CB (*10*, *21*).

Evolved O_2 from JK and CB is inferred to result from decomposition of perchlorate or chlorate salts, based on analogy with other analyses on Mars, on bulk compositions of the JK and CB samples, on the timing of chlorinated hydrocarbon and HCl releases, and on laboratory experiments with perchlorate salts. Perchlorate was definitively identified in soil at the Mars Phoenix landing site (*20*), and O_2 release from the Rocknest aeolian material is roughly consistent with decomposition of Ca-perchlorate (*10*, *21*). The CB sample contains three times the Cl of the JK sample as measured by APXS (1.41 wt % versus 0.4 wt % for CB and JK, respectively) (*7*), and the abundance of O_2 released from CB (splits CB-2 and CB-3) is nearly eight times the abundance from JK (Table 1), suggesting that the substance responsible for the release of O_2 from CB was a perchlorate or chlorate. Similarly, HCl and chlorinated hydrocarbons (chloromethane and dichloromethane) were released in conjunction with O_2 (Figs. 1 and 2, see below), suggesting that Cl and O were hosted by the same compound in CB and JK.

The coincident release of HCl with O_2 in CB is consistent with several types of perchlorate salt (Fig. 2). HCl is evolved during thermal decomposition of Mg- and Fe-perchlorate, caused by reaction between Cl_2 gas and water vapor (*22*–*24*). Thermal decomposition of Ca-perchlorate alone does not yield substantial HCl at temperatures <450°C (*22*, *25*). However, thermal decomposition of Ca-perchlorate in the presence of an Fe-bearing mineral such as pyrrhotite can also yield simultaneous releases of O_2 and HCl (Fig. 3B).

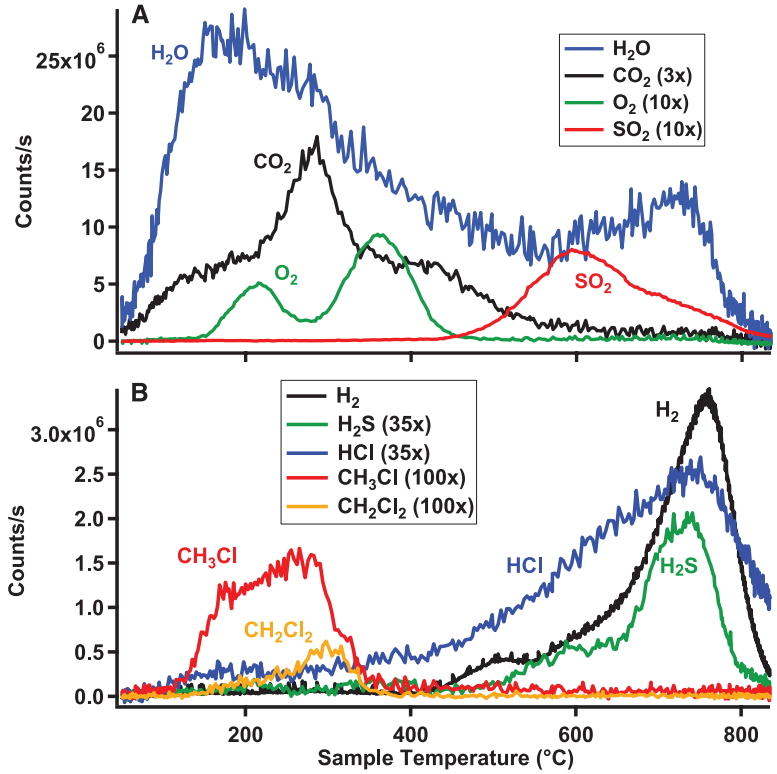

Fig. 1. Evolved gas analysis for a continuous ramp SAM pyrolysis of drill material (<150 μm) from the Sheepbed mudstone JK-4 sample. (**A**) Most-abundant evolved gases [CO_2 has been scaled up 3 times; SO_2 and O_2 have been scaled up 10 times]. (**B**) Evolved gas traces for H_2, H_2S, HCl, CH_3Cl, and CH_2Cl_2 [H_2S and HCl traces have been scaled up 35 times; CH_3Cl and CH_2Cl_2 have been scaled up 100 times]. Isotopologs were used to estimate species that saturated the QMS detector (*m/z* = 12 for CO_2 and *m/z* = 20 for H_2O).

The O_2-release profiles and temperatures for JK and CB do not match exactly those of common perchlorate salts. Although the best matches are with Fe-perchlorates (Fig. 3C), the presence of Fe-oxides/oxyhydroxides may lower the decomposition temperature of perchlorate salts (*26*). Chlorate salts may also be stable on the martian surface (*27*), and mixtures of K-chlorate and hematite can decompose at temperatures consistent with O_2-release temperatures observed in JK and CB (*26*). Other possible sources of the low-temperature O_2 release—e.g., peroxides and superoxide radicals—cannot be ruled out (*28*–*30*).

Evolved CO_2

The CO_2 releases for the JK and CB samples peaked at temperatures below 300°C (Figs. 1A and 2A), distinct from the CO_2 release between 400° and 512°C from the Rocknest aeolian materials (*10*). The CO_2 releases in the Rocknest samples were interpreted to derive largely from carbonates (*10*), and the CO_2 release shoulder around 400° to 450°C in the JK samples could also derive from carbonate minerals, specifically fine-grained Fe/Mg-carbonate (*10*, *24*, *31*). The 400° to 450°C release shoulder is absent from the CB samples. Another possible CO_2 source, given the inferred presence of akaganeite and substantial proportions of perchlorate or chlorate phases in the samples, is that HCl evolved at lower temperatures and then reacted with carbonate minerals (*23*). The onset of evolved HCl is nearly simultaneous with CO_2 releases in JK and CB (Figs. 1 and 2), suggesting that low-temperature acid dissolution and subsequent thermal decomposition of carbonates may be responsible for some of the evolved CO_2 (fig. S2). Total CO_2 evolved is equivalent to <1 wt % carbonate and, if present, carbonates are at abundance below the detection limit by CheMin. Adsorbed CO_2 is an unlikely candidate for the CO_2 peak near 300°C because most adsorbed CO_2 is expected to be desorbed from smectite and palagonite-like material surfaces at temperatures <200°C (*32*). The low-temperature shoulder around 100° to 200°C in JK materials could reflect adsorbed CO_2, although it was not seen in CB materials.

Although there are several possible CO_2 sources in JK and CB materials, the simultaneous evolution of CO_2 and O_2, in conjunction with a possible O_2 inversion (i.e., O_2 consumption) in JK-4 and the similar CO_2 and O_2 releases in CB samples, suggest combustion of C compounds. It is nearly certain that at least some of the CO_2 produced is derived from the combustion of vapor from *N*-methyl-*N*-(*tert*-butyldimethylsilyl) trifluoroacetamide (MTBSTFA, a derivatization agent carried in SAM) and its reaction products that were identified by the EGA and GCMS experiments and adsorbed onto the samples and sample cups inside SAM during sample transfer in Curiosity's sample acquisition and processing system (*10*, *21*, *33*). The background-derived C detected in the blank runs was up to ~120 and 30 nmol of C attributed to MTBSTFA and

dimethylformamide (DMF) (*33*), respectively. If the background was similar for the analyzed samples of the mudstone, another source of C for combustion to CO_2 during pyrolysis is required to account for the >2 μmol of evolved CO_2 (Table 2). The estimated amount of MTBSTFA + DMF C in the blank runs is only 1 to 3% of total evolved CO_2-C from JK and CB analyses. Also, lower amounts of MTBSTFA C (~18 nmol C) and DMF C (~15 nmol C) were detected in the CB-5 analysis (Table 2), suggesting that substantially less MTBSTFA and DMF were available for combustion to CO_2 in this run due to implementation of the MTBSTFA-reduction protocol (*14*). These results indicate that most of the evolved CO_2 from CB is not related to the known terrestrial C background in SAM, and therefore additional C sources are required.

The initial amount of MTBSTFA and DMF C in the JK and CB analyses could have been higher than the levels measured in the empty-cup blank because of additional adsorption of these volatiles to the solid-sample surface area after sample delivery. A triple-sized sample portion (~135 mg of sample) of JK (JK-3) was delivered to SAM to explore the effects of adsorption on measured CO_2 releases. Estimates of the amount of C from MTBSTFA and DMF sources that could contribute to evolved CO_2 for the JK-3 triple-portion sample show that the levels are similar (within error) compared to the single-portion JK sample analyses (column 4 of Table 2), despite the potential for at least three times as much MTBSTFA and DMF adsorption to the sample due to greater surface area. Also, the triple-portion sample evolved 2.4 to 3.5 times as much CO_2 (Table 2). MTBSTFA and DMF C likely contributed to a small portion of the evolved CO_2 (*21*). The order-of-magnitude more C observed as CO_2 in all samples and the near threefold increase in CO_2 observed for the triple portion run further demonstrate that the dominant C source for CO_2 in the JK analyses came from the mudstone itself and not from known background C sources in SAM or Curiosity's sample acquisition and delivery system.

Another possible C source for the evolved CO_2 is combusted martian indigenous and/or exogenous (meteoritic) organic matter in the mudstone. The Sheepbed mudstone has trace-element compositions consistent with a meteoritic contribution that may have delivered 300 to 1200 parts per million (ppm) organic C (*7*) and/or from weathering of igneous material (*34*). Also, metastable partially oxidized weathering products of martian organics of indigenous and/or exogenous origins such as mellitic acid (*35*) may have undergone decarboxylation during analysis in SAM. Laboratory analog experiments using SAM-like instrument conditions where mellitic acid and perchlorate salts were heated together have shown that the primary degradation products detected during pyrolysis are CO_2 and CO (*36*, *37*). If mellitic acid or other benzenecarboxylates were present in Sheepbed, the organic degradation products may have decomposed to CO_2 and other less-volatile degradation products, which could have gone undetected by SAM GCMS under the oven conditions used for the pyrolysis experiments.

Overall, the potential CO_2 sources include combustion of terrestrial organics resident in SAM (for a small portion of the evolved CO_2), low-temperature acid dissolution of martian carbonates, and combustion and/or decarboxylation of indigenous and/or exogenous organic materials.

Evolved SO_2 and H_2S

Sulfur dioxide and H_2S evolved from the JK and CB samples during pyrolysis, and both also evolved from the Rocknest aeolian material (*10*). The release of both reduced and oxidized S volatiles suggests that reduced and oxidized S species were present in all samples, or that redox reactions in the SAM oven affected S speciation. The total abundance of S-bearing gases and the ratio of SO_2/H_2S observed at JK were both <30% of the values measured in Rocknest samples. Abundances of these gases were even lower in CB than in JK, consistent with the lower bulk S composition measured by APXS [1.57 (±0.03) wt % SO_3 for CB compared with 5.52 (±0.21) wt % SO_3 for JK (*7*)].

The evolved SO_2 had a release peak temperature at ~600° to 625°C, with a shoulder at ~675°C (Figs. 1A and 2A). Several mineral sources of S are possible. CheMin detected anhydrite, bassanite, and pyrrhotite in both JK and CB and possible pyrite in JK (*8*). Pyrrhotite and possibly pyrite are candidate S sources for the SO_2 and H_2S releases from CB and JK. The lower-temperature SO_2 and HCl evolutions occurred simultaneously with the release of O_2 in CB (Fig. 2), and two additional SO_2 release peaks were observed in the 500° to 800°C range. Laboratory pyrolysis experiments of mixtures of pyrrhotite and Ca-perchlorate exhibited similar release patterns for SO_2, O_2, and HCl (Fig. 3B); however, the onset temperatures for their release is lower in CB, consistent with a different perchlorate/chlorate salt (i.e., lower O_2 release) or complex chemistry occurring in the SAM ovens that lowers the decomposition temperature of oxychlorine compounds (as discussed above). Thermal decomposition of Ca-sulfate is not likely to have contributed to the SO_2 releases from JK and CB because they typically break down at higher temperatures than the maximum that can be achieved by the SAM oven used in these experiments (>835°C).

Although pyrrhotite and pyrite are candidate S-bearing phases in CB and JK, the evolved SO_2 data are not uniquely diagnostic of these or any specific S-bearing phases. Fe-sulfate minerals

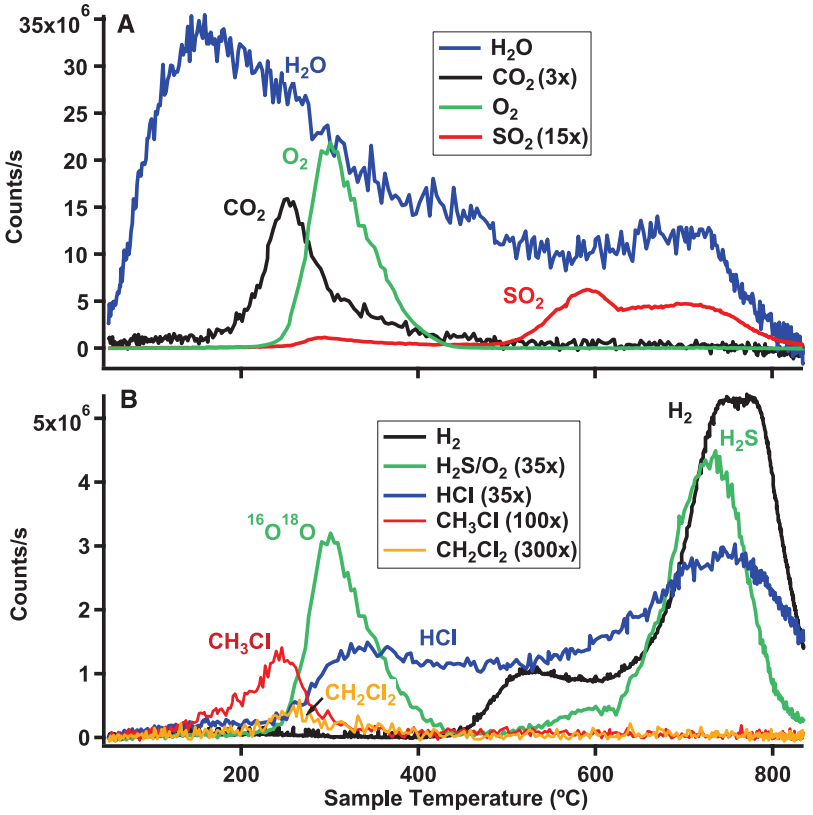

Fig. 2. Evolved gas analysis for a continuous ramp SAM pyrolysis of drill material (<150 μm) from the Sheepbed mudstone CB-2 sample. (**A**) Most-abundant evolved gases [CO_2 and SO_2 counts have been scaled up 3 and 15 times, respectively]. (**B**) Evolved gas traces for H_2, H_2S, HCl, CH_3Cl, and CH_2Cl_2 [H_2S and HCl traces have been scaled up 35 times; CH_3Cl and CH_2Cl_2 have been scaled up 100 and 300 times, respectively]. Isotopologs were used to estimate species that saturated the QMS detector (m/z = 12 for CO_2 and m/z = 20 for H_2O).

will evolve SO_2 at 500° to 800°C under conditions similar to SAM operational conditions. However, formation of Fe-sulfates requires strongly acidic conditions (*38*, *39*), and Sheepbed is interpreted to record depositional and diagenetic environments at near-neutral pH's (*1*).

Evolution of H_2S occurred nearly simultaneously with evolution of H_2 and high-temperature H_2O resulting from the dehydroxylation of the 2:1 phyllosilicate (Figs. 1 and 2). H_2S may be a by-product of the reaction of H_2O with a Fe-sulfide such as pyrrhotite (Fig. 3B); however, it is possible that SO_2 evolved at high temperatures is reduced in the presence of H_2 to H_2S (*40*, *41*). HCl also evolves at higher temperatures (Figs. 1B and 2B), which can react with reduced S phases to form H_2S (*42*, *43*).

Evolved N-Bearing Species

Potential N-bearing compounds evolved from JK and CB include NO, HCN, CH_3CN, ClCN, CF_3CN, and $C_3H_4F_3NO$. Evolved NO [mass/charge ratio (m/z) = 30] in the JK and CB materials had abundances of 129 to 190 nmol and 190 to 389 nmol NO, respectively (Table 1). The abundances of NO in JK and CB blank runs were 70 and 12 nmol, respectively, and the predicted level of N contributed by MTBSTFA and DMF based on background measurements was typically less than 20 nmol N. Hence, the source for the evolved NO appears to be within the mudstone. Other N compounds detected by SAM (HCN, CH_3CN, and ClCN) are present at substantially lower abundances, and they may be contributed by the MTBSTFA and DMF background in the SAM instrument. Both wet chemistry reagents contain one N atom per molecule of reagent. CF_3CN is almost certain to be from decomposition of MTBSTFA because possible sources of F in the martian samples (i.e., fluorapatite) will not decompose in the SAM temperature range. In addition, HCN and CH_3CN have also been identified during laboratory pyrolysis of MTBSTFA and DMF in the presence of perchlorate run under similar operating conditions as SAM (*21*).

Organic Compounds

Pyrolysis of the JK and CB samples led to low-temperature (125° to 350°C) release of chloromethane and dichloromethane that correlated with the release of O_2 and 1,3-bis(1,1-dimethylethyl)-1,1,3,3-tetramethyldisiloxane, a known reaction product of MTBSTFA and H_2O (fig. S3). This correlation suggests that thermal degradation of the O_2 source (most likely an oxychlorine compound, see above) is contributing to chlorination of C phases and/or the release of chlorinated hydrocarbons. Identification and quantification of these trace organic species by their characteristic m/z values in EGA mode was enhanced and confirmed by bulk collection and GCMS identification (*44*) of volatiles on an adsorbent-resin hydrocarbon trap (Fig. 4 and fig. S4). Detection of chlorinated hydrocarbons by SAM in Rocknest samples (*10*, *21*), as well as supporting laboratory EGA and GCMS experiments conducted under SAM-like conditions, have shown that both chloromethane and dichloromethane are produced when MTBSTFA and DMF are heated in the presence of Ca- and Mg-perchlorates (*21*). Therefore, reaction of MTBSTFA and DMF carbon with an oxychlorine compound is a likely source of some of the chloromethane and dichloromethane detected in JK and CB.

Empty-cup blank analyses before each sample set (Rocknest, JK, and CB) showed low chloromethane C abundance (<7 nmol C, including estimated error, via EGA) and no detection of dichloromethane. In comparison to the blanks, single-portion runs of JK and CB consistently showed more abundant chloromethane and dichloromethane C [up to about six times the abundance; range: 21 (± 4) to 66 (±13) nmol C, Table 2], whereas lower amounts of chloromethane and dichloromethane [12 (± 2) nmol C] were released from Rocknest single-portion samples, even though the total MTBSTFA C amounts measured during pyrolysis of Rocknest were similar (within error) to those measured in JK and the CB-1 and CB-2 runs (Table 2). Furthermore, the JK-3 EGA analysis of a triple-portion sample released approximately twice as much chloromethane + dichloromethane [127 (±25) nmol C] as a single-portion JK analysis [38 (±8) to 66 (±13) nmol C], and JK-3 released trichloromethane ($CHCl_3$) and carbon tetrachloride (CCl_4), which were not previously detected in the blank or single-portion JK experimental runs (table S2 and Fig. 4). However, the increase in chlorinated products in JK-3 could also be explained by three times as much sample (i.e., more oxychlorine compounds) compared to the single-portion JK runs. Trichloromethane and carbon tetrachloride were also detected by GCMS in both CB-3 and CB-5 at similar levels (table S2). These data indicate that greater chlorinated hydrocarbon production is associated with the Sheepbed mudstone (compared with the Rocknest aeolian deposit) and with larger sample mass. However, the substantial reduction (~50%) in C abundance from MTBSTFA (and presumably DMF) in the CB-5 experiment compared with CB-3 (fig. S5 and Table 2) was matched by a ~50% drop in chloromethane and dichloromethane detected by EGA [10.2 (±2.0) and 0.7 (± 0.2) nmol C, respectively]. This suggests that

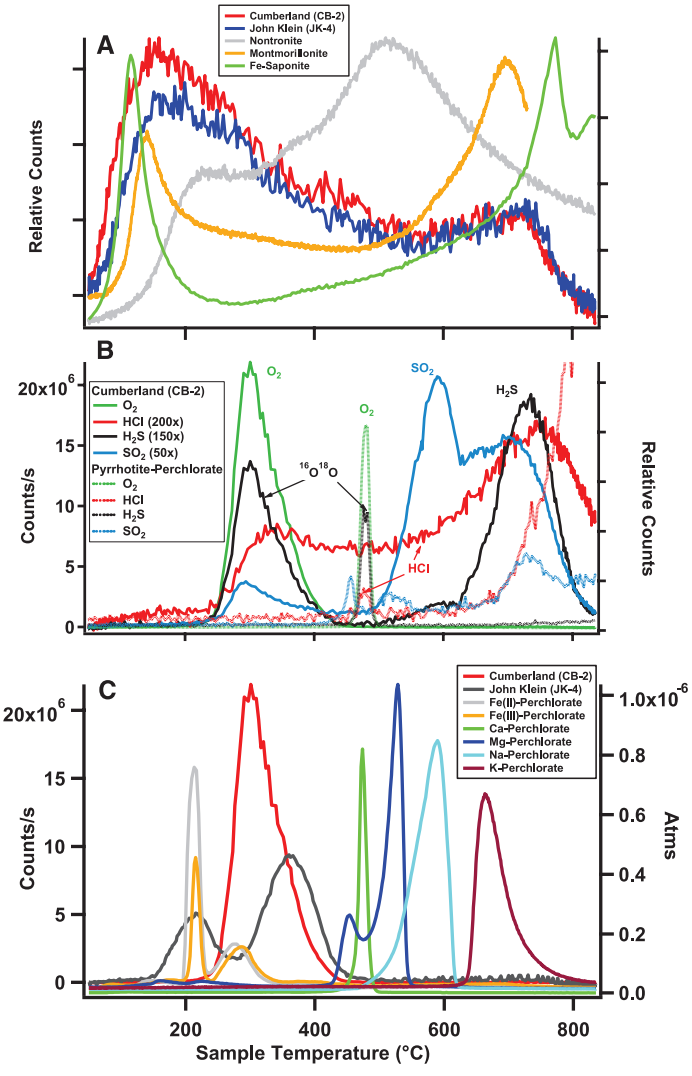

Fig. 3. Major evolved gases from the JK and CB samples compared with EGA of analog minerals under SAM-like oven operating conditions (*14*). (**A**) Evolved H_2O for nontronite, montmorillonite, and saponite compared with JK and CB evolved H_2O. (**B**) Evolved O_2, SO_2, HCl, and H_2S for CB-2 compared with pyrrhotite mixed with a Ca-perchlorate run under SAM-like operating conditions in laboratory experiments (HCl evolution coincides with O_2 release for CB-2 and laboratory pyrrhotite/perchlorate experiments). (**C**) Evolved O_2 for several perchlorate salts compared with JK and CB evolved O_2.

martian organics may not be substantial contributors to these chloromethanes detected in CB samples.

Trace quantities of chloromethane and dichloromethane were also identified by the Viking 1 and 2 lander GCMS instruments (*45*, *46*). The Viking GCMS team attributed the chlorinated hydrocarbons to terrestrial sources including cleaning solvents, although the possibility that some of the chloromethane C was indigenous to Mars was not ruled out (*46*). Unlike SAM, the Viking GCMS instruments did not include an MTBSTFA and DMF wet chemistry experiment. Following the Phoenix perchlorate detection and subsequent laboratory experiments in which Atacama soils mixed with 1 wt % of Mg-perchlorate produced chloromethane and dichloromethane at 500°C, the Viking chloromethane compounds have been attributed to the presence of perchlorates and indigenous organic carbon at the Viking landing sites (*47*). The hypothesis has been challenged (*48*) and debated (*49*).

The EGA and GCMS observations of varying chlorinated hydrocarbon abundances in JK and CB could result from any combination of the following: (i) chlorination of MTBSTFA and DMF or other unknown terrestrial C sources in SAM (instrument background) that were not identified during EGA or GCMS in the empty-cup blank runs; (ii) chlorination of C contamination from the drill and/or sample handling chain; and (iii) chlorination of martian or exogenous C phases in the Sheepbed mudstone.

Terrestrial contamination from the sample handling chain is unlikely because it was scrubbed multiple times with Rocknest scooped material before the first drilled sample at JK (*9*, *10*). The GCMS abundances of chloromethane and dichloromethane measured in JK-4 were similar within error to the abundances of the chlorinated hydrocarbons identified in the second drill sample at CB (CB-2) run under identical conditions (table S2). Therefore, if terrestrial C contamination from the drill was the primary source of C for these chlorinated hydrocarbons in JK-4, their abundances measured in the CB-2 sample should have been reduced compared to JK-4 due to sample scrubbing of hardware surfaces and disposal of the JK sample from the sample processing system. This was not observed. Moreover, swabbed surfaces of Curiosity's sample acquisition and processing system were found to be organically clean before launch (*50*, *51*), and only trace quantities (~0.1 to 0.3 nmol) of perfluoroethene, a known pyrolysis product of Teflon that is within the drill system (*52*), were identified in the JK and CB EGA analyses.

Chlorinated hydrocarbons are likely produced in the SAM oven during heating of samples in the presence of Cl from the thermal decomposition of oxychlorine compounds. Some of the chlorinated hydrocarbon detected at JK and CB may be derived from the sample. The SAM data do not allow us to prove, or disprove, organic C contributions from Sheepbed to evolved chlorinated hydrocarbons and CO_2 from the JK and CB samples. There are no conclusive EGA or GCMS observations of other organic molecules indigenous to the Sheepbed mudstone.

Preservation of Organics

Although the detection and identification of possible organic compounds in the Sheepbed mudstone is complicated by reactions in the SAM oven, the lack of a definitive detection of martian organics suggests that, if organics were deposited in the Sheepbed mudstone, organic alteration and destruction mechanisms may present the single most fundamental challenge to the search for organics on Mars. Some organic compounds are expected on the surface of Mars. Exogenous delivery of meteoritic organics to the martian surface has been estimated as 2.4×10^8 g C/year (*53*) and may have been higher during periods of higher impact flux on the surface. Benzenecarboxylates derived from the oxidation of meteoritic organic matter on Mars could contribute up to 500 ppm organic C by weight in the top meter of the martian regolith (*35*). Abiotic organic matter formed by igneous and/or hydrothermal processes (*34*, *54*) is also expected to be embedded within basaltic minerals where it is protected from chemical oxidants in the environment. Consequently, at least a low concentration of organic compounds is likely in the source material for the Sheepbed mudstone. In addition, the distal fluvial to lacustrine depositional environment of Sheepbed (*1*) makes it a prime site for concentration of organic matter through sedimentary processes (*2*).

If organics were present, evaluating their fate during diagenesis becomes critical for understanding their molecular structures, distribution in sediments, and SAM observations. The JK and CB samples experienced diagenesis, including the alteration of basaltic minerals to smectite and magnetite after deposition (*7*, *8*). Organics may have been released during basaltic mineral alteration, and any reactive organic molecules present may have been incorporated into or adsorbed onto the forming smectite and magnetite. These types of mineral-organic associations could have enhanced

Table 2. Abundances of terrestrial C from *N*-methyl-*N*-(*tert*-butyldimethylsilyl) trifluoroacetamide (MTBSTFA) reaction products and dimethylformamide (DMF) compared with the measured abundances of chloromethane (CM), dichloromethane (DCM) and CO_2 detected during SAM evolved gas analysis (EGA) by the mass spectrometer.

Sample	Total detected MTBSTFA-derived C (μmol)*	Estimate of missing DMF C (μmol)†	Total CM + DCM C (μmol)	Estimated amount of MTBSTFA- and DMF-derived C for combustion (μmol)‡	Total CO_2 (μmol)	Estimated MTBSTFA + DMF C combustion in analysis relative to total CO_2§
JK blank	0.120 ± 0.024	0.030 ± 0.006	0.005 ± 0.001	≈ 0	≈ 0	≈ 0%
JK-1	0.051 ± 0.010	0.013 ± 0.003	0.066 ± 0.013	0.086 ± 0.043	7.0 ± 1.9	1.2 ± 0.7%
JK-2	0.044 ± 0.009	0.011 ± 0.002	0.061 ± 0.012	0.095 ± 0.041	8.1 ± 1.7	1.2 ± 0.5%
JK-3 (3× portion)	0.071 ± 0.014	0.018 ± 0.004	0.127 ± 0.025	0.061 ± 0.048	19.8 ± 4.8	0.3 ± 0.3%
JK-4	0.047 ± 0.009	0.012 ± 0.002	0.038 ± 0.008	0.091 ± 0.041	5.7 ± 1.3	1.6 ± 0.7%
CB blank	0.097 ± 0.019	0.025 ± 0.005	0.006 ± 0.001	≈ 0	≈ 0	≈ 0%
CB-1	0.068 ± 0.014	0.017 ± 0.003	0.025 ± 0.005	0.037 ± 0.041	2.0 ± 0.2	1.9 ± 2.1%
CB-2	0.041 ± 0.008	0.010 ± 0.002	0.022 ± 0.004	0.071 ± 0.034	2.5 ± 0.4	2.8 ± 1.4%
CB-3	0.032 ± 0.006	0.008 ± 0.002	0.021 ± 0.004	0.082 ± 0.032	3.1 ± 0.3	2.7 ± 1.1%
CB-5	0.018 ± 0.004	0.005 ± 0.001	0.011 ± 0.002	ND‖	3.1 ± 0.7	ND‖
RN blank	0.078 ± 0.016	0.020 ± 0.004	0.002 ± 0.001	≈ 0	≈ 0	≈ 0%
RN1-4 (average)	0.058 ± 0.012	0.015 ± 0.003	0.012 ± 0.002	0.025 ± 0.035	9.9 ± 1.2	0.3 ± 0.4%

*Total MTBSTFA C value in μmol determined from the sum of the EGA measured abundances of silylated products: *tert*-butyldimethylsilanol, 1,3-bis(1,1-dimethylethyl)-1,1,3,3-tetramethyldisiloxane, and *tert*-butyldimethylfluorosilane, plus the mole fraction of C from 2,2,2-trifluoro-*N*-methylacetamide in MTBSTFA relative to the sum of the silylated products. †DMF was not identified during pyrolysis by EGA or GCMS. However, the amount of DMF C was estimated from the total measured MTBSTFA C and the molar ratio of DMF/MTBSTFA carbon (0.25) that was originally loaded into the wet chemistry cups, to address a worst-case scenario. ‡Estimated amount of combusted MTBSTFA- and DMF-derived C equals the amount of C in the blank from these sources minus the amount of C from these sources that was observed and calculated for each solid sample run. §Percentage of the total MTBSTFA and DMF carbon in the preceding blank analysis, assumed to be representative of the MTBSTFA and DMF derived carbon available for combustion to CO_2, compared to total CO_2 measured in the sample runs. ‖ND: Values could not be determined because a comparable blank run was not carried out under the same experimental conditions that were used for CB-5.

the early preservation of organic matter. In addition, reducing conditions during deposition, as suggested by the presence of magnetite (*7*), would have favored early preservation. Subsequently, and at any time during burial, oxidants already present in disequilibrium with reduced phases or circulated into the rock may have contributed to the oxidative degradation of organic compounds that were deposited with the sediment or released from the altering igneous minerals. There is no evidence of mineral oxidation associated with the second diagenetic event that precipitated calcium sulfate minerals from fluids into the Sheepbed fracture network (*7*), and the bulk rock remained largely reducing based on the presence of magnetite and pyrrhotite in JK and CB, and possibly pyrite in JK (*8*). However, akaganeite in the samples may reflect oxidative weathering of pyrrhotite, which could indicate exposure of JK and CB to an oxidizing fluid in earlier diagenetic event(s) that may have degraded any organic compounds.

If any organic compounds remained throughout burial, they may have been altered by other mechanisms. The martian surface is subjected to strong ionizing radiation that can alter organic molecules (*55*) depending on the chemical and physical microenvironment of the host sediments (*56*). Ionizing radiation directly breaks chemical bonds in organic molecules and other chemicals, producing a reactive pool of radicals and oxidants (e.g., OH•, H_2O_2, oxychlorine compounds). In the presence of mineral catalysts, these reactants can fully oxidize organic matter to CO, CO_2, and carbonates or produce partially oxidized organics such as acetate, oxalates, and other carboxylates that may survive in a metastable state on Mars (*35*). If exogenous or martian organic matter survived largely intact until removal of the overlying Gillespie sandstone, it may still have degraded or oxidized during surface exposure of the sampling site to ionizing radiation. Therefore, surface-exposure age is also an important variable in the preservation of organics. Alternatively, the organics may have survived all of the martian processing that occurred naturally, only to be oxidized by oxide minerals or oxychlorine compounds at elevated temperatures in the SAM oven or, if sufficiently refractory, survive pyrolysis and pass undetected by SAM, as does most of the kerogen-like material in meteorites.

The complicated story of carbon on Mars is poorly understood. As of sol 370, SAM results support the presence of carbon source(s) in

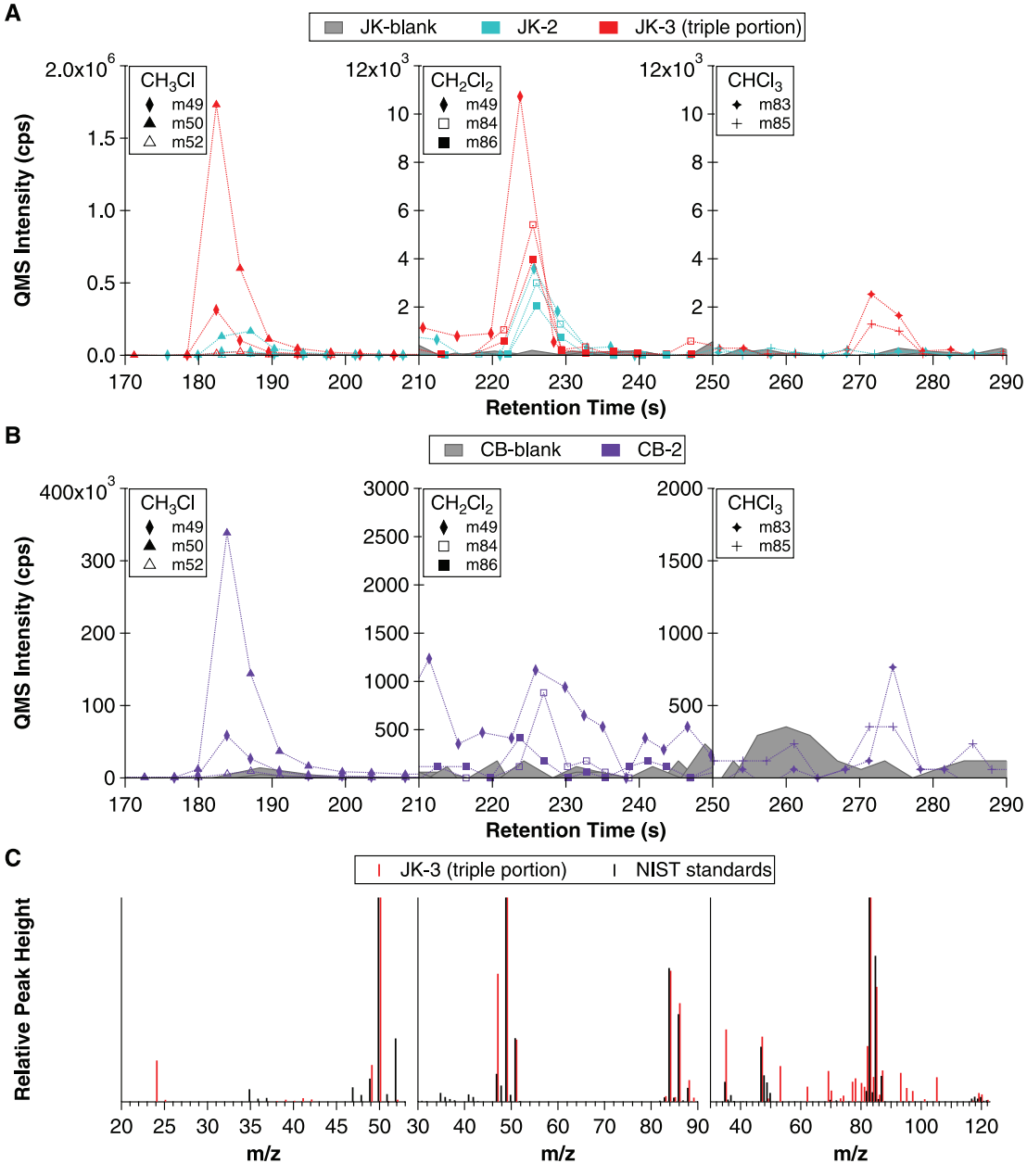

Fig. 4. SAM gas chromatogram of the major *m/z* values of the chlorinated hydrocarbons detected in JK and CB samples (cps, counts/s). (**A**) JK Sample 3 (JK-3; triple portion) compared with JK-2 (single portion) and the JK blank. (**B**) CB Sample 2 (CB-2, single portion) compared with the CB blank. (**C**) The mass spectra generated for the GC peaks detected in JK-3 are shown in red and compared with the mass spectra for chloromethane (CH_3Cl), dichloromethane (CH_2Cl_2), and trichloromethane ($CHCl_3$) in black from NIST/EPA/NIH Mass Spectral Database (*44*).

samples from the Sheepbed mudstone that contribute(s) to the production of chlorinated hydrocarbons and evolved CO_2. There may be organic matter in these samples, but it has not been confirmed as martian.

References and Notes

1. J. P. Grotzinger *et al*., A habitable fluvio-lacustrine environment at Yellowknife Bay, Gale crater, Mars. *Science* **343**, 1242777 (2014). doi: 10.1126/science.1242777
2. R. E. Summons *et al*., Preservation of martian organic and environmental records: final report of the Mars biosignature working group. *Astrobiology* **11**, 157–181 (2011). doi: 10.1089/ast.2010.0506; pmid: 21417945
3. By definition, a mudstone is a fine-grained sedimentary rock composed of 50% or more of particles <62 μm (*4*). The Sheepbed mudstone is composed of ~20% clay minerals and ~30% amorphous materials (*8*).
4. P. E. Potter, J. B. Maynard, P. Depetris, *Mud and Mudstones* (Springer, Berlin, 2005).
5. P. R. Mahaffy *et al*., The Sample Analysis at Mars investigation and instrument suite. *Space Sci. Rev.* **170**, 401–478 (2012). doi: 10.1007/s11214-012-9879-z
6. D. F. Blake *et al*., Characterization and calibration of the CheMin mineralogical instrument on Mars Science Laboratory. *Space Sci. Rev.* **170**, 341–399 (2012). doi: 10.1007/s11214-012-9905-1
7. S. M. McLennan *et al*., Elemental geochemistry of sedimentary rocks at Yellowknife Bay, Gale crater, Mars. *Science* **343**, 1244734 (2014). doi: 10.1126/science.1244734
8. D. T. Vaniman *et al*., Mineralogy of a mudstone at Yellowknife Bay, Gale crater, Mars. *Science* **343**, 1243480 (2014). doi: 10.1126/science.1243480
9. D. F. Blake *et al*., Curiosity at Gale crater, Mars: characterization and analysis of the Rocknest sand shadow. *Science* **341**, 1239505 (2013). doi: 10.1126/science.1239505; pmid: 24072928
10. L. A. Leshin *et al*., Volatile, isotope, and organic analysis of martian fines with the Mars Curiosity rover. *Science* **341**, 1238937 (2013). doi: 10.1126/science.1238937; pmid: 24072926
11. The term ''soil'' is used here to denote any loose, unconsolidated materials that can be distinguished from rocks, bedrock, or strongly cohesive sediments. No implication for the presence or absence of organic materials or living matter is intended.
12. A. S. Yen *et al*., An integrated view of the chemistry and mineralogy of martian soils. *Nature* **436**, 49–54 (2005). doi: 10.1038/nature03637; pmid: 16001059
13. K. H. Nealson, P. G. Conrad, Life: past, present and future. *Philos. Trans. R. Soc. Lond. B Biol. Sci.* **354**, 1923–1939 (1999). doi: 10.1098/rstb.1999.0532; pmid: 10670014
14. Materials and methods are available as supplementary materials on *Science* Online.
15. The mass of each sample portion delivered to SAM was estimated to be 45 ± 18 mg, except for JK-3, where a triple portion (135 ± 31 mg) was delivered to the sample cup. Due to the known presence of the reaction products of MTBSTFA and possibly DMF in the SAM background due to a broken seal (*10*, *21*), the analytical conditions of the first three JK samples were adjusted to boil off these molecules and associated reaction product by heating to 200° to 300°C and holding the temperature for about 20 min. All evolved gases were analyzed directly by the quadrupole mass spectrometer (QMS), but boil-off gases were vented thereafter to simplify GCMS analyses (*14*). The JK-4 sample was run under nominal conditions in which the pyrolysis oven was steadily heated from Mars ambient to ~835°C. Three samples of CB (CB-1, CB-2, and CB-3) were run under the same conditions that were used for the JK-4 sample, i.e., under a continuous temperature ramp starting at Mars ambient conditions. Sample CB-5 SAM cup was preheated to ~120°C and then moved into position directly under the solid sample inlet tube to receive the CB-5 portion from Curiosity's sample delivery system (*14*).
16. R. Gellert *et al*., Initial MSL APXS activities and observations at Gale Crater, Mars. Paper presented at the 44th Lunar and Planetary Science Conference, Houston, TX, 18 to 22 March 2013 (Lunar and Planetary Institute, Houston, TX, 2013).
17. J. L. Campbell *et al*., Quantitative in-situ determination of hydration of bright high-sulfate martian soils. *J. Geophys. Res. Planets* **113**, E06S11 (2008). doi: 10.1029/2007JE002959
18. Only the John Klein sample 4 (JK-4) EGA data set is discussed in the text and shown in Fig. 1. The other three experiments were conducted with a preconditioning boil-off that prevented systematic examination of the temperature of evolution below the boil-off temperature [~300°C (*15*)].
19. The three SAM continuous temperature ramp analyses of the Cumberland material (CB-1, CB-2, and CB-3) revealed similar evolved gas patterns (fig. S1), with variations in the abundances of gases evolved. Only the CB-2 sample is shown in Fig. 2 to represent the Cumberland evolved gas analysis. CB-5 EGA is not shown in this figure because it did not have the sample continuous temperature ramp conditions that were used in the previous three CB runs.
20. M. H. Hecht *et al*., Detection of perchlorate and the soluble chemistry of martian soil at the Phoenix lander site. *Science* **325**, 64–67 (2009). doi: 10.1126/science.1172466; pmid: 19574385
21. D. P. Glavin *et al*., Evidence for perchlorates and the origin of chlorinated hydrocarbons detected by SAM at the Rocknest aeolian deposit in Gale Crater. *J. Geophys. Res.* **118**, 1955–1973 (2013). doi: 10.1002/jgre.20144
22. G. Marvin, L. B. Woolaver, Thermal decomposition of perchlorates. *Ind. Eng. Chem.* **17**, 474–476 (1945).
23. K. M. Cannon, B. Sutter, D. W. Ming, W. V. Boynton, R. Quinn, Perchlorate induced low temperature carbonate decomposition in the Mars Phoenix Thermal and Evolved Gas Analyzer (TEGA). *Geophys. Res. Lett.* **39**, L13203 (2012). doi: 10.1029/2012GL051952
24. B. Sutter *et al*., The detection of carbonate in the martian soil at the Phoenix Landing site: A laboratory investigation and comparison with the Thermal and Evolved Gas Analyzer (TEGA) data. *Icarus* **218**, 290–296 (2012). doi: 10.1016/j.icarus.2011.12.002
25. A. Migdał-Mikuli, J. Hetmańczyk, Thermal behavior of $[Ca(H_2O)_4](ClO_4)_2$ and $[Ca(NH_3O_6](ClO_4)_2$. *J. Therm. Anal. Calorim.* **91**, 529–534 (2008). doi: 10.1007/s10973-007-8511-z
26. W. K. Rudloff, E. S. Freeman, Catalytic effect of metal oxides on thermal decomposition reactions. II. Catalytic effect of metal oxides on the thermal decomposition of potassium chlorate and potassium perchlorate as detected by thermal analysis methods. *J. Phys. Chem.* **74**, 3317–3324 (1970). doi: 10.1021/j100712a002
27. J. Hanley, V. F. Chevrier, D. J. Berget, R. D. Adams, Chlorate salts and solutions on Mars. *Geophys. Res. Lett.* **39**, L08201 (2012). doi: 10.1029/2012GL051239
28. R. C. Quinn, A. P. Zent, Peroxide-modified titanium dioxide: a chemical analog of putative Martian soil oxidants. *Orig. Life Evol. Biosph.* **29**, 59–72 (1999). doi: 10.1023/A:1006506022182; pmid: 10077869
29. A. S. Yen, S. S. Kim, M. H. Hecht, M. S. Frant, B. Murray, Evidence that the reactivity of the martian soil is due to superoxide ions. *Science* **289**, 1909–1912 (2000). doi: 10.1126/science.289.5486.1909; pmid: 10988066
30. A. P. Zent, A. S. Ichimura, R. C. Quinn, H. K. Harding, The formation and stability of the superoxide radical (O_2^-) on rock-forming minerals: Band gaps, hydroxylation state, and implications for Mars oxidant chemistry. *J. Geophys. Res.* **113**, E09001 (2008). doi: 10.1029/2007JE003001
31. P. D. Archer Jr., D. W. Ming, B. Sutter, The effects of instrument parameters and sample properties on thermal decomposition: Interpreting thermal analysis data from Mars. *Planet Sci.* **2**, 2 (2013). doi: 10.1186/2191-2521-2-2
32. J. Jänchen, R. V. Morris, D. L. Bish, M. Janssen, U. Hellwig, The H_2O and CO_2 adsorption properties of phyllosilicate-poor palagonitic dust and smectites under martian environmental conditions. *Icarus* **200**, 463–467 (2009). doi: 10.1016/j.icarus.2008.12.006
33. MTBSTFA (*N*-methyl-*N*-tert-butyl-dimethyl-silyl-trifluoro-acetamide) and DMF have been identified in both empty-cup blank and Rocknest runs. See supplementary materials on *Science* Online.
34. A. Steele *et al*., A reduced organic carbon component in martian basalts. *Science* **337**, 212–215 (2012). doi: 10.1126/science.1220715; pmid: 22628557
35. S. A. Benner, K. G. Devine, L. N. Matveeva, D. H. Powell, The missing organic molecules on Mars. *Proc. Natl. Acad. Sci. U.S.A.* **97**, 2425–2430 (2000). doi: 10.1073/pnas.040539497; pmid: 10706606
36. H. Steininger, F. Goesmann, W. Goetz, Influence of magnesium perchlorate on the pyrolysis of organic compounds in Mars analogue soils. *Planet. Space Sci.* **71**, 9–17 (2012). doi: 10.1016/j.pss.2012.06.015
37. D. W. Ming *et al*., Combustion of organic molecules by the thermal decomposition of perchlorate salts: Implications for organics at the Mars Phoenix Scout landing site. Paper presented at the 40th Lunar and Planetary Science Conference, Houston, TX, 23 to 27 March 2009 (Lunar and Planetary Institute, Houston, TX, 2009).
38. U. Schwertmann, R. M. Cornell, Iron oxides in the laboratory: Preparation and characterization (Wiley-VCH, Weinheim, Germany, 2007).
39. J. M. Bigham, R. W. Fitzpatrick, D. G. Schulze, Iron oxides, in *Soil Mineralogy with Environmental Applications*, J. B. Dixon, D. G. Schulze, Eds. (Soil Science Society of America, Madison, WI, 2002).
40. V. S. Arutyunov *et al*., Kinetics of the reduction of sulfur-dioxide. 3. Formation of hydrogen-sulfide in the reaction of sulfur-dioxide with hydrogen. *Kinet. Catal.* **32**, 1112–1115 (1991).
41. D. Binns, P. Marshall, An abinitio study of the reaction of atomic hydrogen with sulfur-dioxide. *J. Chem. Phys.* **95**, 4940–4947 (1991). doi: 10.1063/1.461710
42. A. A. Baba, F. A. Adekola, O. O. Opaleye, R. B. Bale, Dissolution kinetics of pyrite ore by hydrochloric acid. *J. Appl. Sci. Technol.* **16**, 104–110 (2011).
43. T. R. Ingraham, H. W. Parsons, L. J. Cabri, Leaching of pyrrhotite with hydrochloric acid. *Can. Metall. Q.* **11**, 407–411 (1972). doi: 10.1179/000844372795257575
44. The National Institute of Standards and Technology/Environmental Protection Agency/National Institutes of Health (NIST/EPA/NIH) Mass Spectral Database (NIST SRD Database No. lA, Gaithersburg, MD, 2011) was used to identify chloromethane, dichloromethane, trichloromethane, and tetrachloromethane in GCMS measurements based on spectral lines in the gas chromatograms. The confirmation of these compounds aided in their identification and quantification in EGA.
45. K. Biemann *et al*., Search for organic and volatile inorganic compounds in two surface samples from the chryse planitia region of Mars. *Science* **194**, 72–76 (1976). doi: 10.1126/science.194.4260.72; pmid: 17793082
46. K. Biemann *et al*., The search for organic substances and inorganic volatile compounds in the surface of Mars. *J. Geophys. Res.* **82**, 4641–4658 (1977). doi: 10.1029/JS082i028p04641
47. R. Navarro-González, E. Vargas, J. de la Rosa, A. C. Raga, C. P. McKay, Reanalysis of the Viking results suggests perchlorate and organics at midlatitudes on Mars. *J. Geophys. Res. Planets* **115**, E12010 (2010). doi: 10.1029/2010JE003599
48. K. Biemann, J. L. Bada, Comment on "Reanalysis of the Viking results suggests perchlorate and organics at midlatitudes on Mars" by Rafael Navarro-González *et al*. *J. Geophys. Res.* **116**, E12001 (2011). doi: 10.1029/2011JE003869
49. R. Navarro-González, C. P. McKay, Reply to comment by Biemann and Bada on "Reanalysis of the Viking results suggests perchlorate and organics at midlatitudes on Mars." *J. Geophys. Res.* **116**, E12002 (2011). doi: 10.1029/2011JE003880
50. M. S. Anderson *et al*., *In situ* cleaning of instruments for the sensitive detection of organics on Mars. *Rev. Sci. Instrum.* **83**, 105109 (2012). doi: 10.1063/1.4757861; pmid: 23126806
51. J. E. Eigenbrode *et al*., Dectection of organic constituents including chloromethylpropene in the analysis of the

Rocknest drift by Sample at Mars (SAM). Paper presented at the 44th Lunar and Planetary Science Conference, Houston, TX, 18 to 22 March 2013 (Lunar and Planetary Institute, Houston, TX, 2013).
52. J. E. Eigenbrode *et al.*, Fluorocarbon contamination from the drill on the Mars Science Laboratory: Potential science impact on detecting martian organics by sample at Mars (SAM). Paper presented at the 44th Lunar and Planetary Science Conference, Houston, TX, 18 to 22 March 2013 (Lunar and Planetary Institute, Houston, TX, 2013).
53. G. J. Flynn, The delivery of organic matter from asteroids and comets to the early surface of Mars. *Earth Moon Planets* **72**, 469–474 (1996). doi: 10.1007/BF00117551; pmid: 11539472
54. A. Steele *et al.*, Graphite in the martian meteorite Allan Hills 84001. *Am. Mineral.* **97**, 1256–1259 (2012). doi: 10.2138/am.2012.4148
55. G. Kminek, J. Bada, The effect of ionizing radiation on the preservation of amino acids on Mars. *Earth Planet. Sci. Lett.* **245**, 1–5 (2006). doi: 10.1016/j.epsl.2006.03.008
56. D. M. Hassler *et al.*, Mars' surface radiation environment measured with the Mars Science Laboratory's Curiosity rover. *Science* **343**, 1244797 (2014). doi: 10.1126/science.1244797

Acknowledgments: We are indebted to the Mars Science Laboratory Project engineering and management teams for making this mission possible and enhancing science operations. Much of this research was carried out at the Jet Propulsion Laboratory, California Institute of Technology, under contract with the National Aeronautics and Space Administration (NASA). NASA provided support for the development of SAM. Data from these SAM experiments are archived in the Planetary Data System (pds.nasa.gov). Essential contributions to the successful operation of SAM on Mars and the acquisition of this data were provided by the SAM development, operations, and testbed teams. Development and operation of the SAM and APXS instruments were also supported by funds from the French Space Agency (CNES) and the Canadian Space Agency. Work in the UK was funded by the UK Space Agency. B.L.E., J.L.E., K.F., D.P.G., J.E.G., K.E.M., S.M.M., J.M., P.B.N., and R.E.S. acknowledge funding support from the NASA ROSES MSL Participating Scientist Program.

Supplementary Materials

www.sciencemag.org/content/343/6169/1245267/suppl/DC1
Materials and Methods
Figs. S1 to S6
Tables S1 to S3
References (*57*–*65*)
MSL Science Team Author List

28 August 2013; accepted 12 November 2013
Published online 9 December 2013;
10.1126/science.1245267